COMPUTATION OF LAYERS IN EULERIAN GAS FLOW

P.W.Hemker

CWI, Centre for Mathematics and Computer Science
Amsterdam, The Netherlands

ABSTRACT

A mixed defect-correction iteration process (MDCP) is applied for the implicit numerical solution of steady Euler flows. The iterative procedure gives two solutions that are both 2nd order accurate for smooth parts of the flow, but may differ up to $\Theta(1)$ at discontinuities. In practice it is shown that the discontinuities (shocks and contact discontinuities) are well monitored, and that the influence of the discontinuity on the smooth part of the solution is limited to a few meshwidths. Without stability problems, MDCP can be applied with a straightforward 2nd order scheme such as central differences. A nearly monotonous representation of the thin layers is obtained by application of a 2nd order scheme with a proper flux-limiter. When combined with nonlinear multigrid (FAS-) cycles, a few FAS-MDCP iteration steps are sufficient to determine the two solutions up to truncation-error accuracy.

INTRODUCTION

A Mixed Defect Correction (MDCP) iteration of the form

$$\tilde{L}_h^1 u_h^{(2n+1)} = \tilde{L}_h^1 u_h^{(2n)} - L_h^1 u_h^{(2n)} + f_h , \qquad (1)$$

$$\tilde{L}_h^2 u_h^{(2n+2)} = \tilde{L}_h^2 u_h^{(2n+1)} - L_h^2 u_h^{(2n+1)} + f_h ,$$

was introduced in [1] for the solution of the linear convection diffusion equation. The iterative process (1) has two different limit solutions,

$$u_h^A = \lim_{n \to \infty} u_h^{(2n)} , \qquad (2)$$

$$u_h^B = \lim_{n \to \infty} u_h^{(2n+1)} .$$

With the choice $L_h^2 = \tilde{L}_h^1$, it is derived from (1) that u_h^A satisfies

$$M_h^A u_h^A \equiv \left[L_h^1 + L_h^2 (\tilde{L}_h^2)^{-1} (L_h^2 - L_h^1) \right] u_h^A = f_h , \qquad (3)$$

and for the difference $u_h^B - u_h^A$ we have

$$u_h^B - u_h^A = (\tilde{L}_h^2)^{-1} (L_h^2 - L_h^1) u_h^A . \qquad (4)$$

In [1] it was shown that with an accurate but unstable (central difference) operator L_h^1, with a stable (artificial diffusion) operator $L_h^2 = \tilde{L}_h^1$, and with $\tilde{L}_h^2 = 2.\mathrm{diag}(L_h^2)$, the process (1) converges rapidly and it yields u_h^A and u_h^B that are both 2nd order accurate. Both solutions yield a reasonably sharp representation of thin boundary and interior layers, and these layers can be monitored by the difference $u_h^B - u_h^A$. Here we apply a similar iteration

process to an upwind discretization of the steady Euler equations.

THE PROCESS FOR THE EULER EQUATIONS

We select two different discretizations of the steady (non-isentropic) two-dimensional Euler equations. First, for the stable operator we take the first order upwind discretization $N_h^1(q_h) = 0$, a finite volume scheme with Osher's approximate Riemann solver as described in [4] . Further, for the accurate operator we take a 2nd order discretization $N_h^2(q_h) = 0$, e.g. the central difference scheme (but also other finite volume schemes as described in [2, 5] can be used).

The first order scheme is well suited to represent interior layers (both shocks and contact discontinuities) if they are aligned with the grid. As soon as they are not, the solutions are seriously smeared out. Oblique discontinuities, require schemes with a higher order of accuracy. Here stability problems may arise. The stability of the discrete operator is not only desired to prevent spurious oscillations in the discrete solution, but also to efficiently solve the discrete equations by a multigrid method [4, 3] . To circumvent stability problems during the solution process, defect-correction iteration can be applied. Then, full use can be made of the fast FAS multigrid convergence for the 1st order problem [2] . In this paper we apply the MDCP process in order to stabilize the process further and to obtain additional information.

The non-linear MDCP iteration is described by

$$N_h^1(q_h^{(2n-1)}) = N_h^1(q_h^{(2n-2)}) - N_h^2(q_h^{(2n-2)}) , \qquad (5.a)$$

$$q_h^{(2n)} = q_h^{(2n-1)} - \frac{1}{2}D_h^{-1}(N_h^1(q_h^{(2n-1)})) , \qquad (5.b)$$

where $D_h = D_h(q_h^{(2n-1)}) = \mathrm{diag}(N_h^1(q_h^{(2n-1)}))$ is the non-linear block diagonal operator derived from N_h^1. The diagonal contains 4×4 blocks, that (only) take care of the coupling between the unknowns that are associated with the same cell (finite volume) in the mesh. In this way (5.a) represents a simple defect-correction sweep towards the solution of $N_h^2(q_h) = 0$, by means of the approximate operator N_h^1. The second step, (5.b), describes a damped collective Jacobi relaxation sweep for the solution of $N_h^1(q_h) = 0$. Analogous to (1), the iteration (5) has two limit solutions q_h^A and q_h^B.

These two solutions -computed in alternation- are both 2nd order accurate. The iteration converges with an optimal rate of $\mathcal{O}(h)$ per cycle, for almost all smooth components in the error. Hence, the higher order of accuracy is already obtained in the first iteration steps. For high frequency components, or frequencies along characteristic directions, the method converges more slowly (cf. eq. (6)). Away from layers, the convergence seems independent of the strength of the discontinuities. Starting from the monotonous 1st order approximation, the final solution is approached without significant overshoot in the intermediate results. Depending on the 2nd order scheme used, (nearly) monotonous solutions can be computed in the layers. In practice, for an efficient computation, the iterands $q_h^{(2n-1)}$ in (5.a) are approximated by a single FAS-cycle. This does not harm the convergence of the MDCP iteration

process.

SOME LOCAL MODE ANALYSIS

To get a rough idea of the behaviour of (5), we consider the simple linear, constant coefficient equation

$$u_t = a_1 u_x + a_2 u_y.$$

To its upwind discretization we apply Local Mode Analysis. The discretization stencils are:

$$N_h^1 = \frac{a_1}{h} \left[-1 , 1 , 0 \right] + \frac{a_2}{h} \begin{bmatrix} 0 \\ 1 \\ -1 \end{bmatrix},$$

$$N_h^2 = \frac{a_1}{2h} \left[-1 , 0 , 1 \right] + \frac{a_2}{2h} \begin{bmatrix} 1 \\ 0 \\ -1 \end{bmatrix},$$

$$D_h = \frac{a_1}{h} \left[0 , 1 , 0 \right] + \frac{a_2}{h} \begin{bmatrix} 0 \\ 1 \\ 0 \end{bmatrix}.$$

Hence, we have for a mode $q_{h,\omega}(k,l) = \exp(i(\omega_1 hk + \omega_2 hl))$ the amplification factors

$$\hat{N}_h^2(\omega) = \frac{2i}{h}(a_1 S_1 C_1 + a_2 S_2 C_2),$$

$$\hat{N}_h^1(\omega) = \hat{N}_h^2(\omega) + \frac{2}{h}(a_1 S_1^2 + a_2 S_2^2),$$

$$\hat{D}_h(\omega) = \frac{1}{h}(a_1 + a_2),$$

where $S_m = \sin(\omega_m h_m / 2)$, and $C_m = \cos(\omega_m h_m / 2)$, $m = 1,2$, and we find $\hat{M}_h^A(\omega)$, the amplification factor corresponding with M_h^A, to be equal to

$$\frac{2i}{h}[a_1 S_1 C_1 + a_2 S_2 C_2] \left[1 + \frac{a_1 S_1^2 + a_2 S_2^2}{a_1 + a_2} \right] + \frac{2}{h} \frac{[a_1 S_1^2 + a_2 S_2^2]^2}{a_1 + a_2}.$$

Thus, we see that M_h^A is consistent of order 2 and has a 4th order damping term that is effective for all high frequencies. Further,

$$\hat{u}_h^B - \hat{u}_h^A = \left[\frac{a_1 S_1^2 + a_2 S_2^2}{a_1 + a_2} \right] \hat{u}_h^A,$$

i.e. the difference between u_h^B and u_h^A is large (only) where high frequencies are significant. The modulus of

$$(\hat{N}_h^1(\omega))^{-1} (\hat{N}_h^2(\omega) - \hat{N}_h^1(\omega)) \frac{1}{2}(\hat{D}_h(\omega))^{-1} (\hat{N}_h^1(\omega) - 2\hat{D}_h(\omega)) =$$

$$= \frac{a_1 S_1^2 + a_2 S_2^2}{a_1 + a_2} \cdot \frac{\frac{2}{h}(a_1 C_1^2 + a_2 C_2^2) - \hat{N}_h^2(\omega)}{\frac{2}{h}(a_1 S_1^2 + a_2 S_2^2) + \hat{N}_h^2(\omega)}. \tag{6}$$

determines the convergence of the MDCP iteration. Generally, for low frequencies this is $\mathcal{O}(h)$, but notice the characteristic frequencies ω for which $N_h^2(\omega) \ll \mathcal{O}(h)$!

NUMERICAL RESULTS

To give an impression of the effect of the process (5), we show some results (i) for a problem with a smooth solution, (ii) for a problem with a oblique contact discontinuity, and (iii) for a problem with a oblique shock. The precise description of these problems can be found in [2] .

We use the MDCP process with two different choices of the 2nd order operator, viz. with the central difference scheme (unstable!) and with the 2nd order upwind scheme with the Van Albada limiter. For both instances, for problem (i) the order of accuracy of the method was determined. Therefore, the problem was solved independently on 3 different grids, with resp. 8×16, 16×32 and 32×64 cells, and the corresponding solutions were compared. In all cases the coarsest mesh in the FAS-algorithm was a 2×4 grid. The results are shown in the Tables 1 and 2.

q_h	$||N_h^1(q_h)||$	$||N_h^2(q_h)||$	$||M_h^A(q_h)||$	$||M_h^B(q_h)||$	p
$q_h^{(0)}$	2.7(-3)	8.6(-3)	7.8(-3)	9.2(-3)	1.2
$q_h^{(1)}$	8.0(-3)	2.7(-3)	4.7(-3)	3.5(-3)	2.4
$q_h^{(2)}$	6.7(-3)	3.6(-3)	2.4(-3)	3.7(-3)	2.3
$q_h^{(3)}$	7.5(-3)	1.9(-3)	3.4(-3)	1.4(-3)	1.9
$q_h^{(4)}$	6.5(-3)	2.7(-3)	1.0(-3)	2.8(-3)	1.8
$q_h^{(5)}$	6.6(-3)	1.5(-3)	2.4(-3)	5.2(-4)	2.0
$q_h^{(6)}$	6.0(-3)	2.9(-3)	3.7(-4)	3.0(-3)	1.8
$q_h^{(7)}$	6.6(-3)	1.5(-3)	2.5(-3)	4.2(-4)	1.9
$q_h^{(8)}$	6.0(-3)	2.9(-3)	3.4(-4)	2.8(-3)	1.8
$q_h^{(9)}$	6.6(-3)	1.5(-3)	2.5(-3)	3.4(-4)	1.9
$q_h^{(10)}$	6.0(-3)	2.9(-3)	3.0(-4)	2.8(-3)	1.8

Table 1. Accuracy during the MDCP iteration for problem (i); MDCP with $N_h^2(q_h)$ the central difference scheme; p is the observed order of accuracy. The norms are l_1-norms on the 16×32 grid.
$$M_h^A(q_h) = N_h^2(q_h) - N_h^1(q_h - \frac{1}{2}D_h^{-1}(N_h^1(q_h))) + N_h^1(q_h - \frac{1}{2}D_h^{-1}(N_h^2(q_h))),$$
$$M_h^B(q_h) = N_h^1(q_h) - N_h^1(q_h - \frac{1}{2}D_h^{-1}(N_h^1(q_h))) + N_h^2(q_h - \frac{1}{2}D_h^{-1}(N_h^1(q_h))).$$

The iteration is started with an approximate solution of the 1st order scheme: $N_h^1(q_h) = 0$. From this equation, the approximation $q_h^{(0)}$ is computed by the FMG method, starting on the 2×4 grid, with a single FAS iteration on each level of discretization.

In the tables we see that the process converges rapidly in the first steps of the iteration. Both, $||M_h^A(q_h^{(2n)})||$ and $||M_h^B(q_h^{(2n+1)})||$ decrease by a factor

q_h	$\|N_h^1(q_h)\|$	$\|N_h^2(q_h)\|$	$\|M_h^A(q_h)\|$	$\|M_h^B(q_h)\|$	p
$q_h^{(0)}$	2.7(-3)	9.8(-3)	8.5(-3)	9.8(-3)	1.2
$q_h^{(1)}$	8.7(-3)	5.4(-3)	6.5(-3)	5.0(-3)	2.4
$q_h^{(2)}$	7.3(-3)	5.0(-3)	3.5(-3)	4.9(-3)	2.3
$q_h^{(3)}$	7.4(-3)	3.1(-3)	4.4(-3)	1.9(-3)	2.1
$q_h^{(4)}$	6.2(-3)	3.7(-3)	1.5(-3)	3.6(-3)	1.9
$q_h^{(5)}$	6.8(-3)	2.0(-3)	3.4(-3)	9.5(-4)	2.2
$q_h^{(6)}$	6.1(-3)	3.4(-3)	7.0(-4)	3.2(-3)	1.9
$q_h^{(7)}$	6.7(-3)	1.9(-3)	3.4(-3)	5.5(-4)	2.2
$q_h^{(8)}$	6.0(-3)	3.3(-3)	4.3(-4)	3.1(-3)	2.0
$q_h^{(9)}$	6.7(-3)	1.8(-3)	3.2(-3)	3.8(-4)	2.1
$q_h^{(10)}$	6.0(-3)	3.2(-3)	3.2(-4)	3.0(-3)	1.9

Table 2. Accuracy during the MDCP iteration for problem (i); MDCP with $N_h^2(q_h)$ the upwind one-sided scheme with Van Albada limiter. The meaning of the figures is the same as in Table 1.

of approx. 0.6. In about 3 iteration steps the truncation error accuracy is obtained. Later, for MDCP with the unstable central difference scheme, this convergence factor slows down to 0.8; with the stable one-sided van Albada scheme it remains <0.7 in the first 5 steps.

We notice that, with both schemes, the order of accuracy after the first defect-correction step amply exceeds the expected value of 2. This is a phenomenon observed for a large variety of practical problems as well. As yet it is unsatisfactorily explained.

REFERENCES
1. P.W. HEMKER (1984). Mixed Defect Correction Iteration for the Solution af a Singular Perturbation Problem. *Computing Suppl.5*, 123-145.
2. P.W. HEMKER (1985). *Defect correction and higher order schemes for the multigrid solution of the steady Euler equations*, CWI Report NM-R8523, To appear in Proceedings Multigrid Conference, Cologne, Oct. 1985.
3. P.W. HEMKER, B. KOREN, and S.P. SPEKREIJSE (1986). *A nonlinear multi-grid method for the efficient solution of the steady Euler equations*To appear in the procs of the 10-th ICNMFD.
4. P.W. HEMKER and S.P. SPEKREIJSE (1985). *Multiple Grid and Osher's Scheme for the Efficient Solution of the Steady Euler Equations*, CWI Report NM-R8507, To appear in Appl. Num. Math. 1986.
5. S.P. SPEKREIJSE (1986). *Multigrid solution of monotone second-order discretizations of hyperbolic conservation laws*, CWI-report NM-R8611.
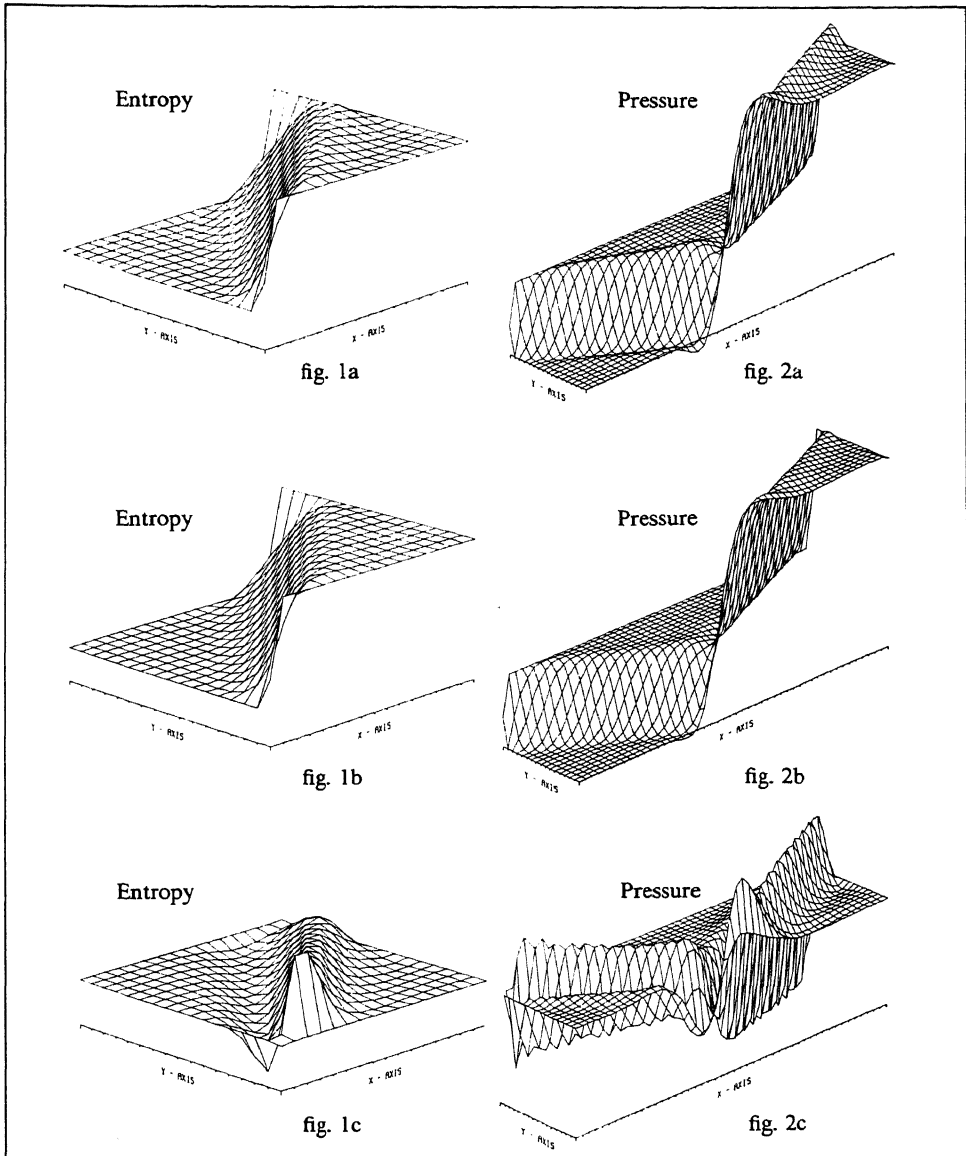
Entropy — fig. 1a

Pressure — fig. 2a

Entropy — fig. 1b

Pressure — fig. 2b

Entropy — fig. 1c

Pressure — fig. 2c

Figure 1. Entropy discontinuity for problem (ii): the oblique contact discontinuity.
(a): $q_h^{(7)}$ with $N_h^2(q_h)$ the central difference scheme.
(b): $q_h^{(7)}$ with $N_h^2(q_h)$ the upwind 2nd order scheme with Van Albada limiter.
(c): $q_h^{(7)} - q_h^{(8)}$, with $N_h^2(q_h)$ the upwind 2nd order scheme with Van Albada limiter ($20 \times$ enlargement of the z-scale).

Figure 2. Pressure discontinuity for problem (iii): the oblique shock.
(a): $q_h^{(8)}$ with $N_h^2(q_h)$ the central difference scheme.
(b): $q_h^{(8)}$ with $N_h^2(q_h)$ the upwind 2nd order scheme with Van Albada limiter.
(c): $q_h^{(7)} - q_h^{(8)}$, with $N_h^2(q_h)$ the central difference scheme ($20 \times$ enlargement of the z-schale).